IASS 2023
July 10–14 Melbourne
Integration of Design and Fabrication

Proceedings of the IASS Annual Symposium 2023
Integration of Design and Fabrication
10–14 July 2023, Melbourne, Australia
Y.M. Xie, J. Burry, T.U. Lee and J. Ma (eds.)

Bridging the gap – A study on foldable tubular bridges

Rupert MALECZEK*, Kiumars SHARIFMOGHADDAM[a], Georg NAWRATIL[a], Clemens PREISINGER[b]

*i.sd / structure and design / department of design / university of Innsbruck
Technikerstraße 21c, UG Süd, 6020 Innsbruck, Austria
rupert.maleczek@uibk.ac.at

[a] Institute of Discrete Mathematics and Geometry & Center for Geometry and Computational Design, TU Wien
[b] Institute of Architecture / University of Applied Arts Vienna

Abstract

Recent investigations on foldable structures and particularly foldable tubes, raise the question if they can be advantageous for the construction of bridge-like beams. Transporting a flat packed structure on site and deploying it there, instead of bringing or constructing the structure on site will have a positive impact on the grey energy. Although a straight beam shows a better performance than a folded one with identical cross-section, the energy saved in transportation might justify the effort. In order to be able to answer this complex question, many steps and investigations need to be done. This paper will answer some questions concerning foldable structures and their geometry-related structural performance. During the ongoing research on T-hedral tubes, the authors developed a strategy to generate flat-foldable tubular beams, on which this particular investigation is based. For the paper at hand a set of these beams, with different cross-sections and variable amount of folds will be compared with respect to their structural performance. The study will focus on their geometry without exact detailing of the hinges or the material thickness. With the help of a parametric model a generic solver [1] and a FEM-module [2] the authors developed a method that evaluates the beams based on their weight after optimisation, in final unfolded state as well as in different configurations during unfolding.

Keywords: structural origami, folding, computational design, bridge building.

1. Introduction

Recent advancements in the field of technical folding and structural origami have led to numerous innovative approaches for various applications. The development and investigation of new folding systems [3][4], along with experiments on a larger scale, have led to the assumption that large scale folding [5] could become more influential in the building industry.

Although new folding algorithms are often presented with freeform shell geometries, the building industry has often higher interest in simple beams or slabs. Elements that can be unfolded on site are often related to disaster relief. One interesting example in this context is the foldable bridge by Ario et al. [6]. Foldable plates structures of rigid material that can be folded on site, are not yet known to be implemented in the building industry.

During the research on foldable polyhedral tubes of the T-hedral type [7] the authors developed two variations of a flat foldable structure, that have a high potential for a beam-like application, as they can be transported in a small package and unfolded on site to their final configuration. Starting from the feasibility of foldable models with only one degree-of-freedom (1-DoF), the investigation towards realisation requires a validation of different folding concepts concerning their stiffness in relation to

their global geometry. In this paper a folded structure is evaluated through its mass after an optimisation process, that reduces the cross-sections of each element in the structure to be as light as possible. Doing so, we can evaluate the global geometry by its weight after optimisation. If certain boundary conditions as e.g. a fixed span are introduced, an algorithm can search for the lightest geometry, and therefore find the best variant.

As geometric and mechanical constraints allow for different geometric solutions, the authors developed a parametric set-up for their particular systems, in order to find optima within the corresponding solution space. After discussing the chosen geometric constraints, the paper focuses on the evaluation of a series of optimisations, to find the best shape for a 20-meter spanning bridge beam.

2. T-hedral Tubes

We aim to design a transformable bridge that exploits the potential offered by polyhedral tubes composed of planar quads (PQ) connected by rotary joints. PQ-meshes in the combinatorics of a square grid with cylindrical topology are generically rigid, but certain geometries allow for a 1-parametric change of the dihedral angles without any deformation of the PQ-panels. This rigid-folding of the whole tubular structure can be controlled by a single actuated rotary joint. Beside this 1-DoF flexion, which can be used for a compact (even flat) folding for transportation, additional properties like a lightweight construction, make these structures suitable to be utilized in kinetic architecture and, in general, transformable design. A close look at the literature [7] on rigid-foldable tubular structures, composed of planar quads where each interior vertex has valence four, reveals that most of the known examples belong to the class of *T-hedral tubes*, which can be generated as follows:

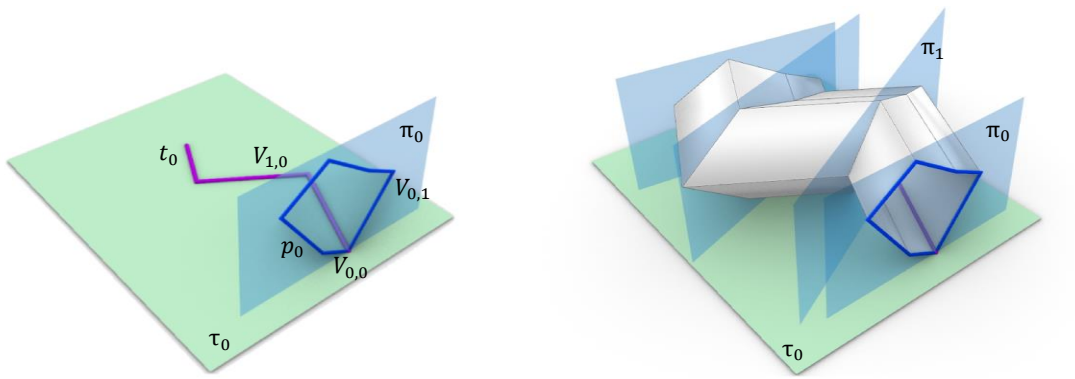

Figure 1. Construction of a T-hedral tube

We start with a planar, closed polygon p_0 located in the plane π_0 and a planar polygon t_0 whose carrier plane is denoted by τ_0 (Figure 1). Moreover, p_0 and t_0 have a common vertex $V_{0,0}$ and the planes π_0 and τ_0 are intersecting orthogonally. The remaining vertices of t_0 and p_0 are denoted by $V_{i,0}$ and $V_{0,j}$, respectively, with $i = 1, \dots, I-1$ and $j = 1, \dots, J-1$. Through each vertex $V_{i,0}$ of t_0 there is a plane π_i orthogonal to the *base plane* τ_0. By a parallel projection of p_{i-1} into the plane π_i along the direction of the polygon edge $V_{i-1,0}V_{i,0}$ of t_0, we obtain the planar polygon $p_i \in \pi_i$. Under this projection the vertices $V_{i-1,j}$ are mapped to $V_{i,j}$. Iteration of this process (for $i = 1, .., I-1$) generates the vertices of the tubular quad-mesh, which has planar trapezoidal faces as the sides $V_{i-1,j-1}V_{i,j-1}$ and $V_{i-1,j}V_{i,j}$ of every quad are parallel. Note that the letter T, stands for trapezoidal, in the nomenclature T-hedral tube. In order that the resulting tube is rigid-foldable the planar closed polygon p_0 has to meet the *loop closure condition* for which we refer to Theorem 3.1 of [7].

It is well-known [8] that T-hedral tubes reach their flexion limits as soon as either a PQ-loop gets completely flat (Figure 2a) or a PQ-strip gets parallel to the base plane (Figure 2c). In the latter case the tube can also transition from one working mode to another. As a consequence, the T-hedral tube can only flex back in such a bifurcation configuration, but the PQ-strip can flip to the opposite side (Figures

2b and 2d). Therefore, this property is also known under the notion of switching [9].

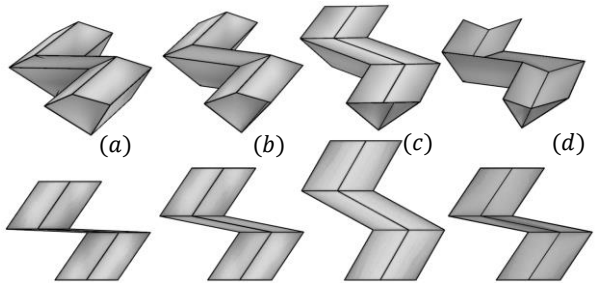

Figure 2. Illustration of the flexion limits (a,c) and working modes (b,d) on basis of a T-hedral tube with deltoidal cross-section in perspective (top) and top views (bottom)

2.1. Specifications for the Bridge Design

To keep the bridge design as simple as possible, we restrict to T-hedral tubes with a quadrilateral cross-section (Figure 3). It can easily be seen that in this case the above-mentioned loop closure condition is only fulfilled if and only if p_0 is

1. a parallelogram,
2. a deltoid with a symmetry line orthogonal to the base plane τ_0,
3. an anti-parallelogram with a symmetry line parallel to the base plane τ_0.

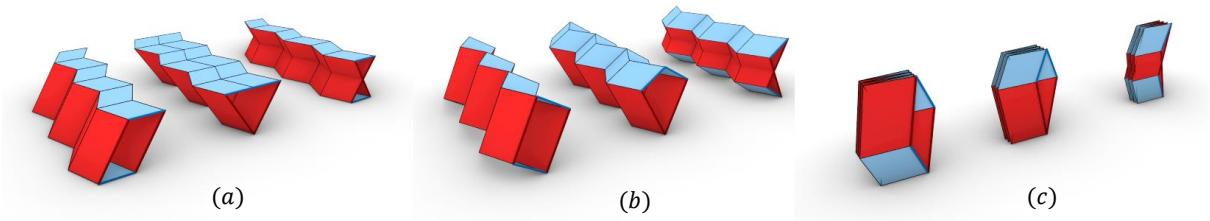

Figure 3. T-hedral tubes with all types of possible quadrilateral cross-sections; parallelogram (left), deltoid (center) and anti-parallelogram (right). (a) unfolded up to the flexion limit, (b) half-folded and (c) flat-folded

In fact, we only deal with cross-sections of cases 1 and 2, because case 3 results in self-intersections for tubular shell models. In addition, we require a repetitive structure of the tubes to ease and cheapen their manufacturing, which yields to the assumption that t_0 is a regular zig-zag. In order to meet our last request of flat-foldability, the planes π_i have to be angle bisectors of t_0 according to [9]. As a consequence, all planes π_i are parallel to the plane π_0 implying T-hedral tubes of the so-called *translational type* (as these tubes are generated by a pure translation from p_0 along t_0).

One can also compose T-hedral tubes by connecting them at PQ-strips in a way that the resulting structure is still rigid-foldable. One can distinguish the following two types of this face-sharing coupling of T-hedral tubes of the translational type [7]. One can put two such tubes together in a way that the corresponding base planes are

- **parallel/identical:** This so-called *aligned-coupling* can easily be constructed by merging two closed polygons p_0^+ and p_0^-, which both fulfil the loop closure condition and share (parts of) a common edge, to a single polygon p_0.
- **not parallel/identical:** This so-called *zipper-coupling* can be achieved by starting with the face-sharing PQ-strip, which has to be a discrete cylinder for the translational type, and chose two base planes in a way that their line of intersection is orthogonal to the cylinder rulings. Note that during the rigid-folding of the zipper tubes the angle enclosed by the base planes changes as illustrated in Figure 7.

Based on these fundamental properties of T-hedral tubes and their couplings, we proceed to explain the

ideas behind the proposed two bridge designs.

2.2. Proposed Two Bridge Designs

Our goal is to achieve a flat bridge deck in the final unfolded state of the structure, which requires to be a flexion limit of at least one involved tube; i.e. the base plane of this tube has to be horizontal. However, as previously mentioned, this is also a bifurcation configuration and it is necessary to prevent the bridge from flexing back (under load). Our focus is on finding purely geometric solutions for blocking the bridge in the final unfolded state.

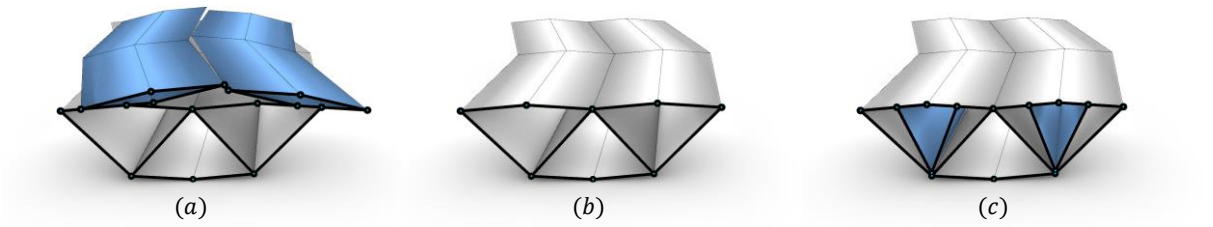

Figure 4. A zig-zag unit of the core structure (b), the zipper-tube solution (a) and the nested deltoid solution (c) close to their final unfolded state

Both presented solutions have the same core structure, which consists of three aligned-coupled deltoidal tubes (see Figure 4b). Note that such an arrangement was also used by Schenk and Guest [10] to construct self-locking metamaterial.

- **Nested deltoid solution**: In this case the bifurcation is prevented by two inner deltoidal tubes, which are aligned-coupled to the outer deltoidal tubes even along two PQ-strips, which is possible due to symmetry (see Figure 4c).
- **Zipper-tube solution**: We zipper-couple two rhombic tubes to the left and right deltoidal tubes of the core structure in a way that in the final unfolded state the rhombic tubes are flat and cover (even extend) the bridge deck (see Figure 4a).

Finally, it should be noted that a flat-foldable bridge structure constructed from zipper-coupled tubes was also presented in Figure 6 of [11]. But neither its deck is flat nor the blocking of the bridge in its finale state was discussed. The latter can for example be achieved by fixing the cross-sections at the bridge end-points to two plates as done in [12]. Moreover, a flat covering of zipper-tubular structures can be obtained by using the concept of smooth sheet attachments [13].

3. Potential Application as a Bridge

As described above, the T-hedral tubes offer interesting behaviour and potential for the building industry as they can be prefabricated in a controlled environment, transported and unfolded into their final spatial configuration on site. For this investigation the two different approaches were analysed for their performance under load, self-weight and their behaviour during the unfolding process, using the FEM-Tool Karamba3D [2] in combination with Galapagos [1] in the Rhino/Grasshopper environment. The authors decided to reduce complexity in this early investigation, and neglected therefore known problems and questions in relation to hinge detailing, material thickness, actuation or materiality.

3.1. Structural Analysis of the Geometries

If folding on site for a bridge should become a potential application two related questions need to be answered: What is the best geometry for the bridge in its final configuration, and what is the best geometry for the unfolding process. In the presented case, the authors also wanted to investigate if rather a nested or the zipper version of the bridge has a better structural performance.

To compare the two options the authors used the FEM-Solver Karamba3D and its ability to optimize cross-sections with given parameters as e.g. maximum admissible deformation. In the presented case

the deflection limit is set to span/300 in accordance to European building codes. As a result, the mass of the structure is optimized. This serves as a performance indicator for comparing design alternatives. The lighter the result the better the geometry. For reducing computational effort, the structures were not analysed as shell structures, but as spatial truss assemblies with the truss-members being aligned to the foldlines and placed as cross bracing thereby modelling the in-plane stiffness of the PQ-panels.

For an investigation on the geometry modelled via shell finite elements, the approach would have been to assign the same weight to the different bridge geometries by controlling the shell thickness and then compare the maximum deflection of the alternative structures. As the folded geometries have in the folded state several layers in the same plane, meshing becomes difficult and slow, resulting in inaccurate structural calculation results. Especially the zipper tube has a high level of complexity, that will be addressed in future investigations.

To have comparable results the bridge spans were defined to be 20 meters having a fixed deck width of 6 meters. The supports were allowed to freely rotate being movable in the bridge's axial direction at one end-point. As truss material hardwood D30 was chosen. The truss-members to be optimised were chosen from a set of cross-sections ranging from 10 to 50 cm edge lengths in 5 cm steps.

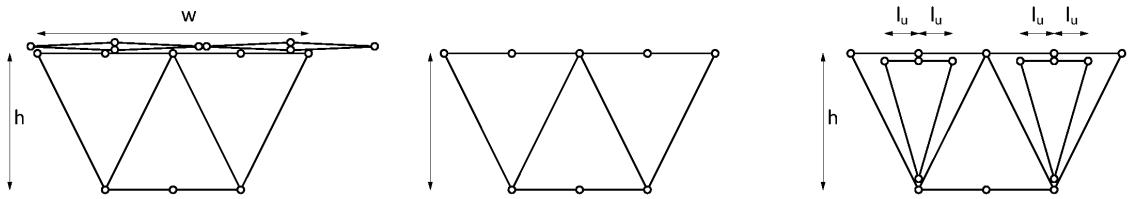

Figure 5. Concept sketch of the variable parameters in section of the zipper tube (left) and the nested solution (right) in its final folded state

The design-alternatives of the bridge had different design parameters that were optimised using Galapagos. As shown in Figure 5, the zipper bridge was variable in the bridge height h, the number of undulations n, the amplitude a of the undulations in x-direction, and the width w of the core structure. The nested bridge was variable in the bridge height h, the number of undulations n, the amplitude a of the undulations in x-direction, and the upper length l_u of the inner deltoid in relation to the total length.

Figure 6. Concept sketch of the two bridge concepts the zipper tube (left) and the nested solution (right) in its final folded state

The structures were optimised for different load cases and in different folding states. The bridges in final state where optimised under self-weight and for a live load of 6kN/m² on the bridge deck. During the (un)folding process the structures were only optimised for self-weight. It was assumed that the bridge would not be folded as a cantilever, but rather as a simply supported beam. This can be achieved with cranes on each side.

3.2. Optimisation Results

As the cross-section optimisation in combination with the Galapagos solver necessitates long computation times the maximum amount of undulations was limited to four, and the deviation was limited to the range 0.25 to 7.5 meters, with a step size of 0.25 meters.

Under live load both solutions converge to the maximum allowed height of the system that was limited to two meters, having a maximum number of 4 undulations, using the minimum allowed deviation of 0.25 meters. The ten best results of both geometries have heights in the upper bound of the height domain and feature the maximum number of undulations. The high number of undulations is linked to the reduction of buckling lengths of the truss members, that result in better structural performance. The nested bridge is 1.4 tons heavier, and therefore less performative under live load as compared to the zipper geometry (cf. Table 1 and Figure 8).

Table 1. The best results of the two systems under live load

live load : 6 kN / m2	NESTED BRIDGE									
	1	*2*	*3*	*4*	*5*	*6*	*7*	*8*	*9*	*10*
FinalStateHeight [m]	2.0	1.9	1.8	2.0	2.0	1.9	1.9	1.9	1.8	1.8
lu	0,25	0,25	0,25	0,33	0,08	0,33	0,17	0,08	0,33	0,08
a - amplitude [m]	0,25	0,25	0,25	0,25	0,25	0,25	0,25	0,25	0,25	0,25
n - undulation	4	4	4	4	4	4	4	4	4	4
Mass [kg]	**10748**	**10789**	**10838**	**10845**	**10889**	**10896**	**10913**	**10918**	**10949**	**10987**

live load : 6 kN / m2	ZIPPER BRIDGE									
	1	*2*	*3*	*4*	*5*	*6*	*7*	*8*	*9*	*10*
FinalStateHeight [m]	2.0	2	1,9	2	1,9	1,9	2	1,9	1.9	2,0
w - width [m]	4,1	4	4	4,2	4,1	4,2	3,7	3,9	4,3	3,6
a - amplitude [m]	0,25	0,25	0,25	0,25	0,25	0,25	0,25	0,25	0,25	0,25
n - undulation	4	4	4	4	4	4	4	4	4	4
Mass [kg]	**9367**	**9399**	**9431**	**9461**	**9466**	**9566**	**9571**	**9580**	**9590**	**9592**

Under self-weight the total mass difference between the best results of the nested and zipper variant remains constant. Similar to the calculation with live load the mass difference amounts to 1.4 tons. Both systems tend towards the lower end of the possible predefined height range. The number of undulations switches from 4 to 2, but the amplitude is kept at the absolute minimum allowed (cf. Table 2).

Table 2. The best results of the two systems under self-weight

self-weight	NESTED BRIDGE									
	1	*2*	*3*	*4*	*5*	*6*	*7*	*8*	*9*	*10*
FinalStateHeight [m]	1	1	1	1.0	1.8	1.3	1.3	1.8	1.3	1.4
lu	0,08	0,17	0,25	0,17	0,25	0,75	0,83	0,33	0,50	0,58
a - amplitude [m]	0,25	0,25	0,25	0,25	0,5	0,25	0,25	0,75	0,75	0,5
n - undulation	2	2	2	2	2	2	2	2	2	2
Mass [kg]	**7183**	**7197**	**7214**	**7442**	**7463**	**7502**	**7526**	**7547**	**7551**	**7561**

self-weight	ZIPPER BRIDGE									
	1	*2*	*3*	*4*	*5*	*6*	*7*	*8*	*9*	*10*
FinalStateHeight [m]	1,2	1	1,3	2	1,5	1,5	2	1.5	1.9	1,7
w - width [m]	2	2	2,5	2,1	2,7	2,6	2,3	2,5	2,3	2,7
a - amplitude [m]	0,25	0,25	0,25	0,25	0,25	0,25	0,25	0,25	0,25	0,25
n - undulation	2	2	2	2	2	2	2	2	2	2
Mass [kg]	**5806**	**5806**	**5903**	**5904**	**5905**	**5908**	**5912**	**5912**	**5916**	**5917**

According to the intended eraction method of unfolding of the structure on site, one investigation was focusing on the optimisation with regards to the series of folding states. As different configurations feature different speeds of folding and unfolding, the folding ratio is defined to be between 0 and 1, where 1 corresponds to the fully unfolded state, and 0 to the fully folded package that has a total

thickness of 1.5 meters. This number constitutes an estimation, since material thickness and hinge detailing will probably not allow for smaller package sizes.

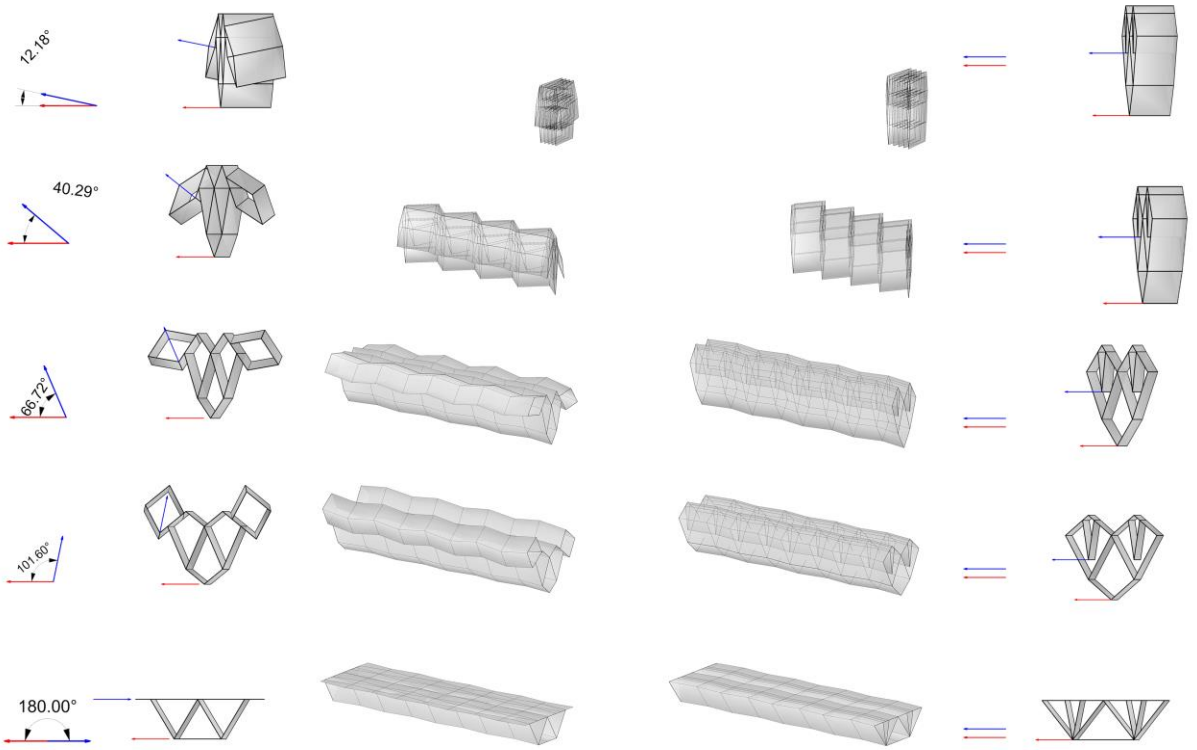

Figure 7. The unfolding sequence from top to bottom of the zipper bridge (left) and the nested bridge (right) with the correspondent angles of the deltoid's base planes. From top to bottom the configurations correspond to the folding ratios 0, 0.25, 0.5, 0.75 and 1.

The folding sequence was split into 4 steps: 0.75, 0.50, 0.25 and 0, respectively. As the entire system is rigidly foldable, the position of each planar quad is exactly defined. Each step has been optimised as a single state, with the endpoints being simply supported.

The results show (cf. Tables 3 and 4), that for the motion states the structural height converges towards the lowest third of the allowable range, whereas for the three best results the optimised height takes on the minimum height possible. The number of undulations is in almost all cases two, its amplitude being 0.25 for most variants. The total mass of both structures is similar and ranges from 7350 kg to 8650 kg. The extreme undulation in the smallest possible folded state leads to an increase in weight for both structures. While the nested bridge has a similar weight in all states, the zipper bridge features a weight increase of 1/3 compared to the case of only self-weight applied. As the folded package represents the transportation case, the latter results are not considered to govern the actual design. For transportation and placement on site necessitate additional manipulation tools which depend on the available technical means.

Table 3. The best results of the nested bridge during motion states

self-weight [0.75]	NESTED BRIDGE									
	1	*2*	*3*	*4*	*5*	*6*	*7*	*8*	*9*	*10*
FinalStateHeight	1	1	1	1	1,1	1,1	1	1,1	1,1	1,2
inner lu	0,8	0,8	0,8	0,8	0,8	0,8	0,8	0,8	0,8	0,8
Deviation	0,25	0,33333	0,41667	0,5	0,25	0,33333	0,58333	0,41667	0,5	0,25
n-undulation	2	2	2	2	2	2	2	2	2	2
Mass	**7352,49**	**7330,07**	**7337,11**	**7346,39**	**7351,18**	**7355,35**	**7357,74**	**7361,95**	**7370,8**	**7378,36**
self-weight [0.50]	NESTED BRIDGE									
	1	*2*	*3*	*4*	*5*	*6*	*7*	*8*	*9*	*10*
FinalStateHeight	1	1.1	1.0	1.2	1.0	1	1.2	1.1	1.1	1.0
inner lu	0,1	0,1	0,2	0,1	0,2	0,1	0,2	0,2	0,1	0,2
Deviation	0,25	0,5	0,25	0,25	0,25	0,5	0,25	0,25	0,5	0,5
n-undulation	2	2	2	2	2	2	2	2	2	2
Mass	**7379**	**7405**	**7406**	**7433**	**7438**	**7444**	**7463**	**7466**	**7468**	**7470**
self-weight [0.25]	NESTED BRIDGE									
	1	*2*	*3*	*4*	*5*	*6*	*7*	*8*	*9*	*10*
FinalStateHeight	1	1	1.6	1.2	1.3	1.4	1	1.1	1	1.2
inner lu	0,1	1,1	0,5	0,8	0,8	0,7	0,9	0,8	0,8	0,8
Deviation	0,25	0,25	0,25	0,5	0,5	0,5	0,25	0,25	0,5	0,75
n-undulation	2	2	2	2	2	2	3	3	3	2
Mass	**7402**	**7421**	**7741**	**8056**	**8068**	**8126**	**8343**	**8350**	**8463**	**8643**

Table 4. The best results of the zipper bridge during motion states

self-weight [0.75]	ZIPPER BRIDGE									
	1	*2*	*3*	*4*	*5*	*6*	*7*	*8*	*9*	*10*
FinalStateHeight	1	1.,1	1,2	1	1,3	1,1	1	1,2	1	1
DriveThrough	5,0	5,0	5,0	4,9	5,0	4,9	5,1	4,9	4,3	5,2
Deviation	0,25	0,25	0,25	0,25	0,25	0,25	0,25	0,25	0,25	0,25
num undulation	2	2	2	2	2	2	2	2	2	2
Mass	**7505,31**	**7514,64**	**7526,52**	**7530,98**	**7537,18**	**7540,18**	**7551,05**	**7553,15**	**7554,67**	**7558,7**
self-weight [0.50]	ZIPPER BRIDGE									
	1	*2*	*3*	*4*	*5*	*6*	*7*	*8*	*9*	*10*
FinalStateHeight	1	1	1	1	1,1	1	1,1	1,1	1,1	1,2
DriveThrough	4,20	4,1	4	3,9	4,2	3,8	4,1	4	3,9	4,2
Deviation	0,25	0,25	0,25	0,25	0,25	0,25	0,25	0,25	0,25	0,25
num undulation	2	2	2	2	2	2	2	2	2	2
Mass	**7587,49**	**7590,78**	**7593,05**	**7597,15**	**7600,38**	**7601,9**	**7603,77**	**7606,17**	**7610,37**	**7614,06**
self-weight [0.25]	ZIPPER BRIDGE									
	1	*2*	*3*	*4*	*5*	*6*	*7*	*8*	*9*	*10*
FinalStateHeight	1,2	1,1	1	1,2	1,3	1,4	1	1.1	1,2	1
DriveThrough	2,70	4,5	4,5	4,5	4,5	4,5	4,5	4,5	4,5	4,3
Deviation	0,25	0,75	0,75	0,75	0,75	0,75	1,5	1,5	1,5	0,25
num undulation	2	2	2	2	2	2	2	2	2	3
Mass	**7773,32**	**7878,28**	**7889.58**	**7890,35**	**7906,21**	**7922,26**	**8007,02**	**8019,59**	**8030,62**	**8082,65**

3.2. Additional Comparisons

If we compare the individual optimised solutions in all states, it turns out that we can differentiate between two sets of results: All variants optimised under self-weight have varying but comparable outcomes in all considered states (during folding under self-weight). When adding live loads to the structural models the optimized mass doubles or triples. Comparing solutions under live load to the states during unfolding, one sees, that the optimised mass is only in the fully folded, initial state higher.

Tables 5 and 6 show mass and displacement values calculated via Karamba3D before and after the cross-section optimisation.

Table 5. The best result of each state (red), investigated in all other states of the nested bridge

NESTED BRIDGE						
	Best Load	Best Eigen	Best 0,75	Best 0,5	Best 0,25	Best 0,00
FinalStateHeight	2,00	1	1	1	1	1,70
lu	0,25	0,08	0,25	0,08	0,08	0,83
a -Amplitude	0,25	0,25	0,25	0,25	0,25	0,75
n-undulation	4,00	2,00	2,00	2,00	2,00	2,00
Load [1]						
Mass	**10 462,95**	**19 728,45**	**18 898,83**	**19 728,45**	**19 728,45**	**16 348,59**
disp orig	5,58	9,53	9,31	9,53	9,53	7,74
disp	3,80	6,48	6,34	6,48	6,48	5,25
Self [1]						
Mass	**8 782,70**	**7 183,00**	**7 089,88**	**7 076,07**	**7 076,07**	**7 449,59**
disp orig	0,90	2,16	2,17	2,15	2,15	1,43
disp	0,66	1,60	1,61	1,59	1,59	1,06
Self [0.75]						
Mass	**9 155,70**	**7 437,20**	**7 325,49**	**7 437,20**	**7 437,20**	**7 726,34**
disp orig	0,40	0,66	0,68	0,66	0,66	1,20
disp	0,29	0,49	0,51	0,49	0,49	0,89
Self [0.5]						
Mass	**9 388,39**	**7 362,91**	**7 385,19**	**7 362,91**	**7 362,91**	**7 743,81**
disp orig	0,43	0,92	0,79	0,92	0,92	1,50
disp	0,32	0,68	0,58	0,68	0,68	1,11
Self [0.25]						
Mass	**9 238,39**	**7 385,82**	**7 382,45**	**7 385,82**	**7 385,82**	**8 453,49**
disp orig	1,83	1,28	1,25	1,28	**1,28**	4,93
disp	1,36	0,95	0,93	0,95	**0,95**	3,65

Table 6. The best result of each state (red), investigated in all other states of the zipper bridge

ZIPPER BRIDGE						
	Best Load	Best Eigen	Best 0,75	Best 0,5	Best 0,25	Best 0,00
FinalStateHeight	2,0	1,2	1	1	1	1
w - width	4,1	2	5	4,2	2,7	5,7
a - Amplitude	0,25	0,25	0,25	0,25	0,25	0,25
n-undulation	4	2	2	2	2	2
Load [1]						
Mass	**9 366,88**	**18 534,53**	**19 767,91**	**19 052,24**	**21 119,28**	**20 187,31**
disp orig	6,15	11,61	9,71	9,50	12,48	9,33
disp	4,14	7,88	6,41	6,46	8,49	6,36
Self [1]						
Mass	**6 843,16**	**5 805,52**	**6 016,25**	**6 026,54**	**5 881,13**	**6 091,97**
disp orig	0,74	5,43	2,45	2,36	4,34	2,55
disp	0,55	4,02	1,81	1,75	3,22	1,89
Self [0.75]						
Mass	**9 040,99**	**7 846,78**	**7 505,31**	**7 596,45**	**7 636,65**	**7 629,54**
disp orig	0,58	2,58	1,41	1,32	2,21	1,95
disp	0,43	1,91	1,04	0,98	1,64	1,45
Self [0.5]						
Mass	**9 031,67**	**7 619,46**	**7 632,51**	**7 587,49**	**7 682,78**	**7 659,92**
disp orig	0,56	6,00	0,98	1,00	3,00	1,11
disp	0,42	4,44	0,73	0,74	2,22	0,82
Self [0.25]						
Mass	**9 008,20**	**7 779,17**	**7 656,30**	**7 615,00**	**7 807,11**	**7 801,47**
disp orig	1,39	7,21	1,01	1,84	1,94	2,00
disp	1,03	5,34	0,75	1,36	1,43	1,48

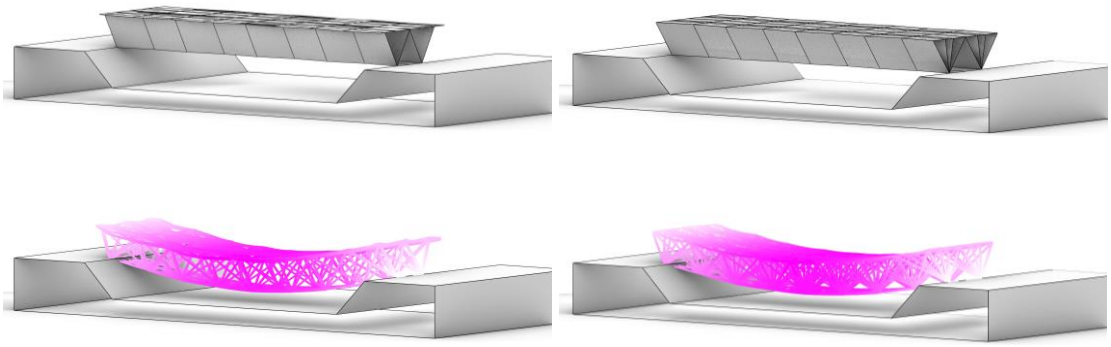

Figure 8. The zipper solution (left) and the nested solution (right) and their deformation under live load

4. Conclusion

The investigation shows that the zipper bridge option has advantages over the nested one in unfolded and final state. Although the zipper tubes are more rigid during the unfolding motion, the nested solution is in some states more efficient. The better performance seems to be linked to the fact that the zipper geometry allows for a slight cantilever of the bridge deck, that reduces the entire surface area and therefore the weight of the core structure.

The investigation shows that the bridge in its smallest possible package state behaves unstable. The reason for this behaviour requires additional investigations, to assess possible solutions to this problem. It can be assumed, that this small transportable package will require special treatment in the course of the erection process.

5. Outlook

This investigation constitutes a starting point for more detailed investigations on bridges based on T-hedral tubes. The presented results are promising and will be followed up by additional research.

In a further study the focus will be on the support conditions during unfolding. Using cantilevering instead of simply supported conditions, one has to control vertical deflections similarly to the analysis presented in [14]. This approach will require multi-objective optimisation to include additional objective functions as e.g. introduced by hinge design, support method, and positioning during unfolding. Another focus is the change from a repetitive pattern of the structural elements to a non-repetitive one that might be adapted for better motion and structural behaviour.

Obviously, future investigations should be refined by using shell elements instead of a simplified beam? model. The simulation problems encountered for the smallest foldable package state suggest a more detailed investigation in relation to the panel thickness, hinge solution, actuation and the temporary support during motion. If these problems can be solved, it is planned to build scaled demonstrators in a consecutive step.

Acknowledgements

The research is supported by grant F77 (SFB “Advanced Computational Design”) of the Austrian Science Fund FWF.

References

[1] D. Rutten, “Navigating Multi-Dimensional Landscapes in Foggy Weather as an Analogy for Generic Problem Solving,“ *Proceedings of the 16th International Conference on Geometry and Graphics*, pp. 826-839, 2014.

[2] C. Preisinger, "Linking Structure and Parametric Geometry," *Architectural Design*, vol. 83, pp. 110-113, 2013.

[3] K. Suto and K. Tanimichi, "Crane," Food4Rhino, 15 06 2022. [Online]. Available: https://www.food4rhino.com/en/app/crane. [Zugriff am 15 06 2022].

[4] R. Foschi, R. Kraft, R. Maleczek, K. Mundilova and T. Tachi, "Comparison of computational curved folding design methods," Proceedings of the IASS annual Conference 2020/21, Inspiring the next generation, pp. 2720-2730, 2021.

[5] R. Maleczek, G. Stern, A. Metzler and C. Preisinger, "Large Scale Curved Folding Mechanisms," *Impact: Design with all senses*, C. Gengnagel, O. Baverel, J. Burry, M. Ramsgaard Thomsen und S. Weinzier, Hrsg., Berlin, Springer, pp. 539-553, 2019.

[6] I. Ario, M. Nakazawa, Y. Tanaka, I. Tanikura and S. Ono, "Development of a prototype deployable bridge based on origami skill, " *Automation in Construction*, vol. 32, pp. 104-111, 2013.

[7] K. Sharifmoghaddam, R. Maleczek and G. Nawratil, "Generalizing rigid-foldable tubular structures of T-hedral type," arXiv:2301.09969, 2023.

[8] R. Sauer and H. Graf, "Über Flächenverbiegung in Analogie zur Verknickung offener Facetten-flache," *Mathematische Annalen*, vol. 105, pp. 499–535, 1931.

[9] E.T. Filipov, G.H. Paulino and T. Tachi, "Origami tubes with reconfigurable polygonal cross-sections," *Proceedings of the Royal Society A: Mathematical, Physical and Engineering Sciences*, vol. 472, Article ID. 20150607, 2016.

[10] M. Schenk and S.D. Guest, "Geometry of Miura-folded metamaterials," *Proceedings of the National Academy of Sciences of the United States of America*, vol. 110, pp. 3276–3281, 2013.

[11] E.T. Filipov, T. Tachi and G.H. Paulino, "Origami tubes assembled into stiff, yet reconfigurable structures and metamaterials," *Proceedings of the National Academy of Sciences of the United States of America*, vol. 112, pp. 12321–12326, 2015.

[12] Z. Wo, J.M. Raneses and E.T. Filipov, "Locking Zipper-Coupled Origami Tubes for Deployable Energy Absorption," *Journal of Mechanisms and Robotics*, vol. 14, Article ID. 041007, 2022.

[13] D.C. Webb, E. Reynolds, D.M. Halverson and L.L. Howell, "Asymmetric Zipper-Coupled Tubes and Smooth Sheet Attachments in the Design of Deployable Space-Filling Mechanisms," *Journal of mechanisms and Robotics*, vol. 16, Article ID. 011004, 2024.

[14] E.T. Filipov, T. Tachi and G.H. Paulino, "Coupled origami tubes for stiff deployable cantilevers," *Proceedings of the ASME 2019 International Design Engineering Technical Conferences and Computers and Information in Engineering Conference*, vol. 5B, Article ID. V05BT07A023, 2019.